2009 International Symposium on Nonlinear Theory and its Applications
NOLTA'09, Sapporo, Japan, October 18-21, 2009

Bifurcation of Simplified Boost Converters for Constant/Controlled Input

Takashi Maeda† and Toshimichi Saito†

†EE Dept., Hosei University, Koganei, Tokyo, 184-0002 Japan; tsaito AT hosei.ac,jp

Abstract—This paper presents a simple switched dynamical systems based on boost converters for constant/controlled input. The input is represented by a current-controlled voltage source and is connected to the output through an inductor and switches. The dynamics is described by piecewise linear systems with nonlinear switching rules and the analysis can be integrated into a one dimensional return map. Using the return map, we have investigated interesting bifurcation phenomena between stable periodic behavior and chaos.

1. Introduction

Switched dynamical systems (SDS) are nonlinear systems consisting of sub-dynamics of continuous state variables and switching rules that define connection of the sub-dynamics. The SDS relates to many important engineering systems including switching power converters, analog-to-digital converters and spiking neurons [1]-[3]. The switching can cause interesting bifurcation phenomena. Analysis of such SDS can contribute to basic design of efficient engineering systems and development of bifurcation theory.

This paper presents a simple SDS that can be regarded as a simplified model of boost converters with constant/controlled input. The input is represented by a linear current-controlled voltage source (CCVS) and is connected to the output through an inductor and switches. As a parameter varies, the CCVS is changed from the constant source to the controlled source and the SDS is changed from a simplified model of dc-dc converters [9] to that of the photovoltaic systems [4, 5]. Effects of the parameter relate to various problems, e. g., design of the maximum power point tracker [5] - [8].

The circuit dynamics is described by piecewise linear systems with nonlinear switching rules and the analysis can be integrated into a one dimensional return map [9, 10]. Using the map, we have investigated bifurcation for the CCVS parameter. Especially, we have found an interesting bifurcation form a long periodic orbit to chaos that can not be observed in the case of dc-dc converters. Basic bifurcation sets can be calculated precisely.

It should be noted that mainstream in analysis of photovoltaic systems are small signal steady state analysis. Chaotic dynamics and global stability have not been analyzed sufficient so far. This results provides basic information to realize stable operation of switching power converters and for detailed analysis of complex bifurcation phenomena [9].

2. The Switched Dynamical System

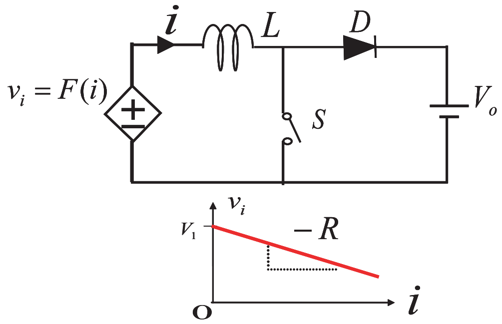

Figure 1: Switched Dynamical Systems

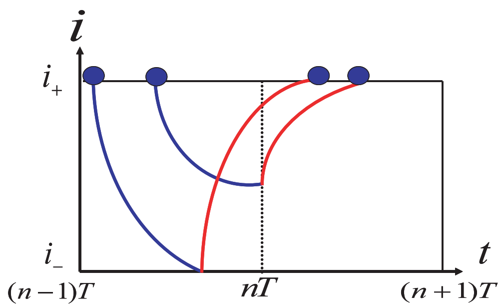

Figure 2: Switching rule and definition of the phase map

Fig. 1 shows the SDS based on the boost converter. The circuits includes the linear CCVS characterized by

$$F(i) = -Ri + V_1 \tag{1}$$

The case $r = 0$ and $r > 0$ correspond to the dc and controlled inputs, respectively. The circuit can be either of the following two states:

State 1: S conducting and D blocking
State 2: S blocking and D conducting

As shown in Fig. 2, the switch S and diodes D are controlled by both inductor current i and periodic clock with period T:

Rule: State 1 → State 2: when $i = i_+$
State 2 → State 1: when $i = i_-$ or $t = nT$

where i_+ and i_- are the upper and lower thresholds of the inductor current i, respectively. The circuit dynamics is described the following equation and the switching rule.

$$L\frac{di}{d\tau} = \begin{cases} F(i) & \text{for State 1} \\ F(i) - V_o & \text{for State 2} \end{cases} \quad (2)$$

Since $(i_+ - i_-) > 0$, the circuit can not be the discontinuous conduction mode where both S and D are blocking. We have assumed that all the circuit elements are ideal and the switchings are instantaneous as routine of circuit analysis [9]. The output voltage V_o corresponds to the RC load of the converter in our simplification method [9]: the voltage regulation is assumed to be achieved in high frequency modulation. If such simplification is not available, the circuit has two or more state variables and precise analysis is very hard.

In order to extract essential parameters, we derive a dimensionless equation. We define the following dimensionless variables and parameters:

$$\tau = \frac{t}{T},\ x = \frac{i - I_-}{I_+ - I_-},\ r = \frac{RT}{L}$$
$$a = \frac{1}{I_+ - I_-}\left(\frac{V_1}{r}\right),\ b = \frac{1}{I_+ - I_-}\left(\frac{V_1}{r} - \frac{V_0}{r}\right)$$

Using these, Eq. (2) and the switching rule are transformed into

$$\frac{dx}{d\tau} = \begin{cases} -rx + a & \text{for State1} \\ -rx - b & \text{for State2} \end{cases} \quad (3)$$

Rule: State 1 → State 2: when $x = 1$
State 2 → State 1: when $x = 0$ or $\tau = n$.

Fig. 3 shows typical waveforms calculated by exact piecewise solution. As parameter varies, the SDS exhibits various periodic and chaotic behavior. Especially, stable periodic orbit (SPO) in Fig. 3 (c) is period 2 and is impossible the SDS of dc-dc converters.

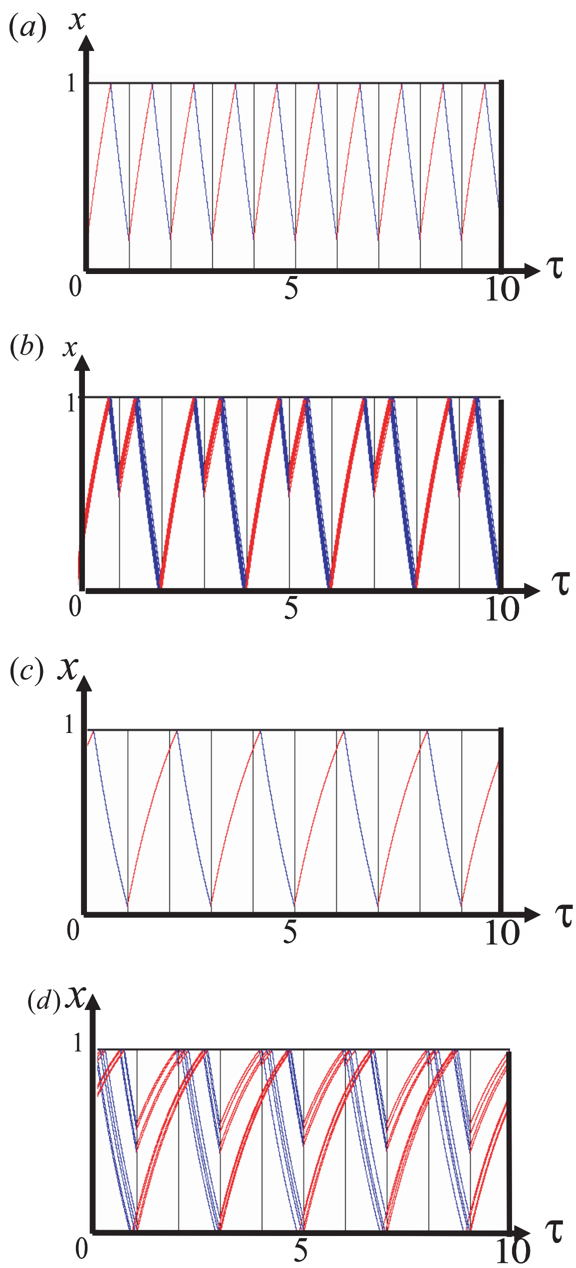

Figure 3: Typical waveforms for $r = 0.7$. (a) SPO for $a = 1.9$ and $b = 1.5$. (b) Chaos for $a = 1.608$ and $b = 1.446$. (c) SPO for $a = 1.206$ and $b = 0.828$. (d) Chaos for $a = 1$ and $b = 0.846$.

3. The return map and stability

In order to analyze bifurcation phenomena, we derive the return map. As shown in Fig. 4, let τ_n denote n-th switching moment at which x reaches the upper threshold 1. At time τ_n, State 1 is changed into State 2 and x decays for the lower threshold 0. If x reaches 0 or the next clock pulse with period 1 arrives, State 2 in changed into State 1 and x reaches 1 again at time τ_{n+1}. Since the τ_n determines τ_{n+1}, we can define 1-D return map $\tau_{n+1} = F(\tau_n)$ from positive reals to itself. Performing elemental geometrical calculation of the PWL orbits, we can obtain explicit formulation of the map:

$$\tau_{n+1} = F(\tau_n)$$
$$= \begin{cases} \tau_n - \frac{1}{r}\left(\ln\left(\frac{b}{r+b}\right) - \ln\left(\frac{a}{a-r}\right)\right) & \text{for } 0 < \tau_n \le \tau_D \\ \frac{1}{r}\ln\left(\frac{r}{r-a}\left(\left(1+\frac{b}{r}\right)e^{r(\tau_n - 1)} - \frac{a+b}{r}\right)\right) + 1 & \text{for } \tau_D \le \tau_n < 1 \end{cases} \quad (4)$$

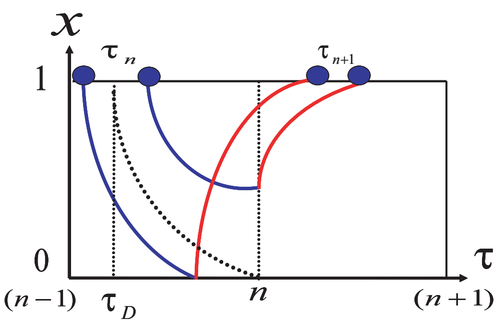

Figure 4: Definition of return map

where $\tau_D = n + \frac{1}{r} \ln \frac{b}{r+b}$. For simplicity, we introduce phase variable $\theta_n = \tau_n$ mod 1. Using the phase, the return map can be reduced into the phase map from $I \equiv (0, 1)$ to itself:

$$\theta_{n+1} = f(\theta_n) \equiv F(\theta_n) \bmod 1 \,. \quad (5)$$

Fig. 5 shows typical phase maps for $r > 0$. As parameters vary a fixed point p_1 is born via tangent bifurcation (see (a) to (c)). The fixed point p_1 corresponds to SPO with period 1 in Fig. 3 (a). The fixed point loses its stability and is changed into chaotic orbit via tangent bifurcation as shown in (d). The second fixed point p_2 is born as (e). It corresponds to SPO with period 2 in Fig. 3 (c). The second fixed point p_2 is changed into chaotic orbit via tangent bifurcation as shown in (f). Here we define several bifurcation sets.

- $B_1 = \{(a, b, r)|F(\theta_D) = \theta_D + 1\}$: the first tangent bifurcation set on which the break point θ_D is a fixed point of the phase map f and corresponds to periodic orbit with period 1.
- $B_2 = \{(a, b, r)|F(\theta_D) = \theta_D + 2\}$: the second tangent bifurcation set on which the break point θ_D is a fixed point of the phase map f and corresponds to periodic orbit with period 2.
- $B_{p1} = \{(a, b, r)|Df(p_1) = -1\}$: the first period doubling bifurcation set on which the first fixed point p_1 loses its stability. $Df(p_1)$ denotes the slope of f at p_1.
- $B_{p2} = \{(a, b, r)|Df(p_2) = -1\}$: the second period doubling bifurcation set on which the second fixed point p_2 loses its stability.
- $B_D = \{(a, b, r)|\theta_D = 0\}$: a parameter set on which the break point θ_D disappears.

Using the exact piecewise solution, these parameter sets can be calculated precisely. The results are illustrated in Fig. 6.

In order to consider effects of the parameter r, we show bifurcation diagram for $r = 0$ and typical phase maps in Figs. 7 and 8. The case $r = 0$ corresponds to dc-dc converters and their detailed analysis results can be found in

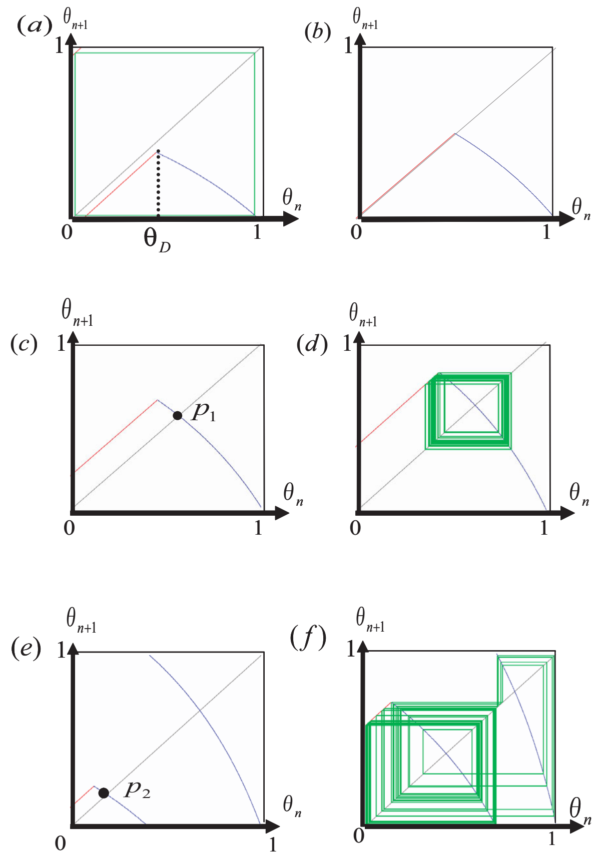

Figure 5: Phase map for $r = 0.7$ (a) $a = 2.9$ and $b = 1.5$.(b)$a = 2.35$ and $b = 1.65$.(c)$a = 1.9$ and $b = 1.5$.(d)$a = 1.608$ and $b = 1.446$.(e)$a = 1.206$ and $b = 0.828$.(f)$a = 1.00$ and $b = 0.846$.

[10]. Note that the phase map is piecewise linear and the second periodic doubling bifurcation set B_{p_2} does not exist. As shown in the figures, the first fixed point p_1 is born via tangent bifurcation and changed into chaotic orbit via period doubling bifurcation. The second fixed point p_2 can be born but can not be stable because the map is piecewise linear. That is, second or more period doubling is possible only if $r > 0$. More detailed analysis is in progress.

4. Conclusions

We have analyzed basic dynamics of a simplified model of boost converter whose input is represented by the CCVS. As a parameter vary, the CCVS is changed from the dc source to the controlled source and the SDS is changed from a simplified model of the dc-dc converter to the MPPT. Using the piecewise exact solution and the phase map, basic bifurcation between periodic attractor and chaos has been investigated.

Future problems are many, including detailed analysis of bifurcation phenomena, measurement of conversion efficiency, and experimental confirmation of typical phenomena.

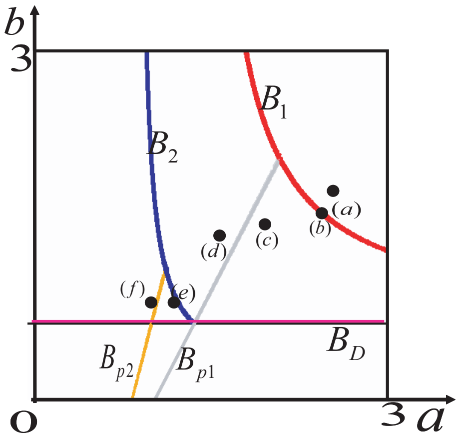

Figure 6: Bifurcation diagram for r = 0.7.

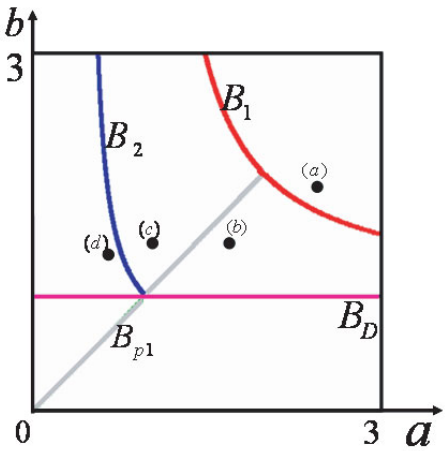

Figure 7: Bifurcation diagram for r = 0.

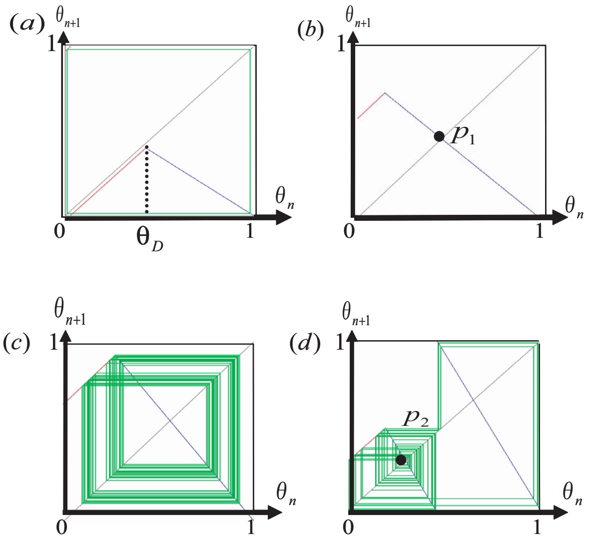

Figure 8: Phase map for r = 0 (a) a = 2.4 and b = 1.746.(b)a = 1.374 and b = 1.18.(c)a = 1.086 and b = 1.374.(d)a = 0.672 and b = 1.248.

References

[1] T.Saito, H.Torikai and W.Schwarz, Switched dynamical systems with double periodic inputs: an analysis tool and its application to the buck-boost converter, IEEE Trans. Circuits Syst. I, 47, 7, pp.1038-1046, 2000.

[2] C. K. Tse and M. di Bernardo, Complex behavior in switching power converters, Proc. IEEE, 90, pp. 768-781, 2002.

[3] S. Banerjee and G. C. Verghese, eds., Nonlinear Phenomena in Power Electronics: Attractors, Bifurcations, Chaos, and Nonlinear Control, IEEE Press, 2001.

[4] Y. H. Lim and D. C. Hamill, Chaos in spacecraft power systems. Electron. Lett. 35, 9, pp. 510-511, 1999.

[5] M. Veerachary, T. Senjyu and K. Uezato Neural-Network-Based Maximum-Power-Point Tracking of Coupled-Inductor Interleaved-Boost-Converter-Supplied PV System Using Fuzzy Controller, IEEE Trans. Ind. Electron., 50, 4, pp. 749-758, 2003.

[6] K. K. Tse, B. M. T. Ho, H. S.-H. Chung and S. Y. Ron Hui, A Comparative Study of Maximum-Power-Point Trackers for Photovoltaic Panels Using Switching-Frequency Modulation Scheme, IEEE Trans. Ind. Electron., 51, 2, pp. 410-418, 2004.

[7] N. Femia, G. Lisi, G. Petrone, G. Spagnuolo and M. Vitelli, Distributed Maximum Power Point Tracking of Photovoltaic Arrays: Novel Approach and System Analysis, IEEE Trans. Ind. Electron., 55, 7, pp. 2610-2621, 2008.

[8] N. D. Benavides and P. L. Chapman, Modeling the Effect of Voltage Ripple on the Power Output of Photovoltaic Modules. IEEE Trans. Ind. Electron., 55, 7, pp. 2638-2643, 2008.

[9] T. Saito, T. Kabe, Y. Ishikawa, Y. Matsuoka and H. Torikai, Piecewise constant switched dynamical systems in power electronics, Int'l J. of Bifurcation and Chaos, 17, 10, pp. 3373-3386, 2007.

[10] D. Kimura and T. Saito, Stability analysis of switched dynamical systems for effective switching strategy of DC/DC converters, Proc. IEEE/IECON, pp. 965-970, 2008.